Characterization of the Vajont landslide (North-Eastern Italy) by means of reflection and surface wave seismics

Lorenzo Petronio [a], Jacopo Boaga [b,*], Giorgio Cassiani [b]

[a] IRI - OGS Trieste, Trieste, Italy
[b] Dipartimento di Geoscienze, Università di Padova, Padova, Italy

ARTICLE INFO

ABSTRACT

The mechanisms of the disastrous Vajont rockslide (North-Eastern Italy, October 9, 1963) have been studied in great detail over the past five decades. Nevertheless, the reconstruction of the rockslide dynamics still presents several uncertainties, including those related to the accurate estimation of the actual landslide mass. This work presents the results of a geophysical characterization of the Vajont landslide body in terms of material properties and buried geometry. Both aspects add new information to the existing dataset and will help a better understanding of the rockslide failure mechanisms and dynamics. In addition, some general considerations concerning the intricacies of landslide characterization can be drawn, with due attention to potential pitfalls. The employed techniques are: (i) high resolution P-wave reflection, (ii) high resolution SH-wave reflection, (iii) controlled source surface wave analysis. We adopted as a seismic source a vibrator both for P waves and SH waves, using vertical and horizontal geophones respectively. For the surface wave seismic survey we used a heavy drop-weight source and low frequency receivers. Despite the high noise level caused by the fractured conditions of the large rock body, a common situation in landslide studies, we managed to achieve a satisfying imaging quality of the landslide structure thanks to the large number of active channels, the short receiver interval and the test of appropriate seismic sources. The joint use of different seismic techniques help focus the investigation on the rock mass mechanical properties. Results are in good agreement with the available borehole data, the geological sections and the mechanical properties of the rockmass estimated by other studies. In general the proposed approach is likely to be applicable successfully to similar situations where scattering and other noise sources are a typical bottleneck to geophysical data acquisition on landslide bodies.

© 2016 Elsevier B.V. All rights reserved.

1. Introduction

The Vajont rockslide (North-Eastern Italy) is one of the best known and most tragic natural disaster induced by human activity, and is one of the largest catastrophic slope failures of the past century. On the 9th of October 1963 about 270 million m^3 of limestone, mudstones and marls slid from Mount Toc, in the North-Eastern part of the Veneto Region, Italy, into a large artificial reservoir built few years earlier for electricity production. The impact induced a water wave that overtopped the dam (the tallest in Europe at that time) and killed more than 2000 people in the valley of the Piave river downstream (Fig. 1). This landslide is one of the most famous erroneous estimation in geology history, due not only to its tragic consequences, but also to its particular behavior. The catastrophic failure was in fact preceded by a phase of accelerating creep, clearly related to the reservoir water level variation tests. The appearance of an M-shaped tension crack on

the southern slope of Mount Toc, 1 km wide and 2.5 km long, foretold in fact the oncoming failure several months before the event (Müller, 1987). Despite this clear evidence, technicians and experts of the time remained anchored to the existing studies (Boyer, 1913; Dal Piaz, 1928) hypothesizing the presence of a very large and slow moving landslide that could be controlled during the reservoir operations. The total cost of the tragedy exceeded US$16 million of the time and the US$100 million dam and relative reservoir were abandoned just after been built (Superchi et al., 2010).

The Vajont landslide was intensively studied immediately after the tragedy by several international research teams (e.g. Carloni and Mazzanti, 1964a, 1964b; Frattini et al., 1964; Kiersch, 1964; Müller, 1964, 1968). Over the past decades other contributions came from new field observations (Semenza, 1986; Mantovani and Vita-Finzi, 2003). In spite of these research efforts, the landslide morphological and structural controls, in terms of failure mechanisms and dynamics, are not yet completely understood. The very large literature on the Vajont case (see e.g. Superchi et al., 2010 for a recent review) shows that most of the recent studies for re-evaluating the failure mechanisms were conducted on the basis of old borehole data, re-elaborated with

* Corresponding author.
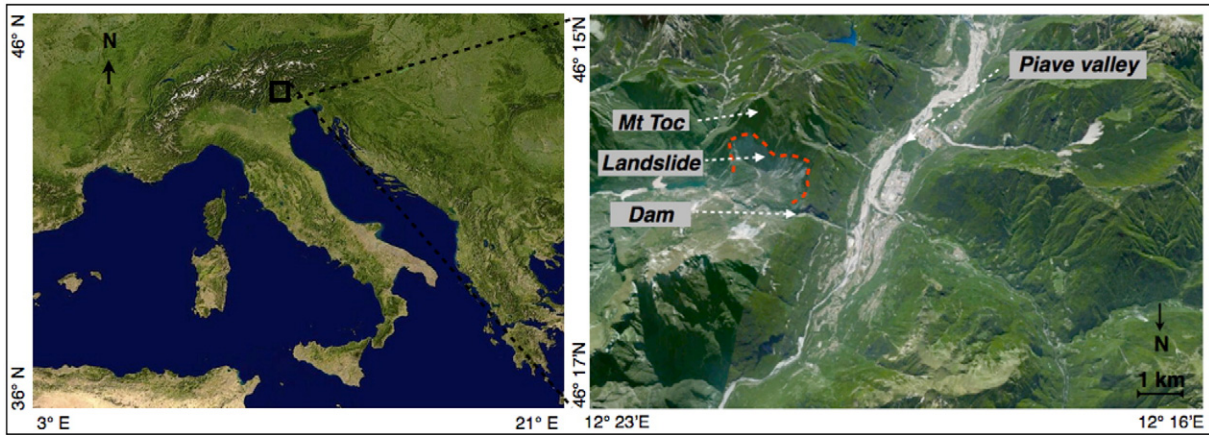 *E-mail address:* jacopo.boaga@unipd.it (J. Boaga).

Fig. 1. The Vajont Mount Toc landslide and the Piave river valley, N–E Italy. The dotted red line shows the extent of the landslide detachment area.

new methods and techniques for rock mass analyses (Hendron and Patton, 1985; Semenza and Ghirotti, 1998; Semenza, 2010).

Modern investigations of landslides have increasingly adopted non-invasive (geophysical) techniques (for a review, see e.g. Jongmans and Garambois, 2007). Among the most commonly used methods are: geoelectric (Suzuki and Higashi, 2001; Lapenna et al., 2005; De Vita et al., 2006; Nguyen et al., 2007; Piegari et al., 2009; Tric et al., 2010) and seismic (Heincke et al., 2006; Stucchi and Mazzotti, 2009; Romdhane et al., 2011; Gance et al., 2012; Samyn et al., 2012; Malehmir et al., 2013). More limited use has been made of GPR, some-times in combination with other methods (e.g. Carpentier et al., 2012), possibly as a consequence of a depth of penetration too limited to reach targets of interest in landslide studies (e.g., the slip surface). The use of multiple geophysical techniques and interdisciplinary data integration has been advocated and practiced with variable degrees of success, using geoelectrics and GPR (e.g. Göktürkler et al., 2008), geoelectrics and electromagnetics (e.g. Godio and Bottino, 2001; Schmutz et al., 2009), geoelectrics and seismics (e.g. Jongmans et al., 2000; Godio et al., 2006; Heincke et al., 2010; Grandjean et al., 2011) and even wider multi-disciplinary approaches (e.g. Bievre et al., 2012).

While of course geometries and geological structures vary widely be-tween case studies, and so vary the specific requirements of non-invasive characterization, some general guidelines can be drawn, particularly for the most commonly used methods, i.e. seismic and geoelectric:

- Seismic can provide key information on landslide structure, provid-ed that resolution and penetration issues are properly tackled in an environment made difficult by scattering induced by the damaged soil/rock sliding body.
- Seismic can also provide information on the mechanical properties of the rock mass, of course with some important caveats: (a) P-wave velocity may depend more on water-saturated conditions than on rock mechanical properties; (b) elastic moduli derived from seismics are inherently small-strain moduli, thus their direct translation into rockmass elastic properties or even worse mechan-ical resistance properties shall be approached with great care.
- Geoelectric is generally easier to deploy along steep hillslopes and can give, like seismic does, information on the system's structure. However, one should always recall that the presence of water is the single most important affecting soil and rock electrical proper-ties. As water is also a critical factor in slope stability issues, this
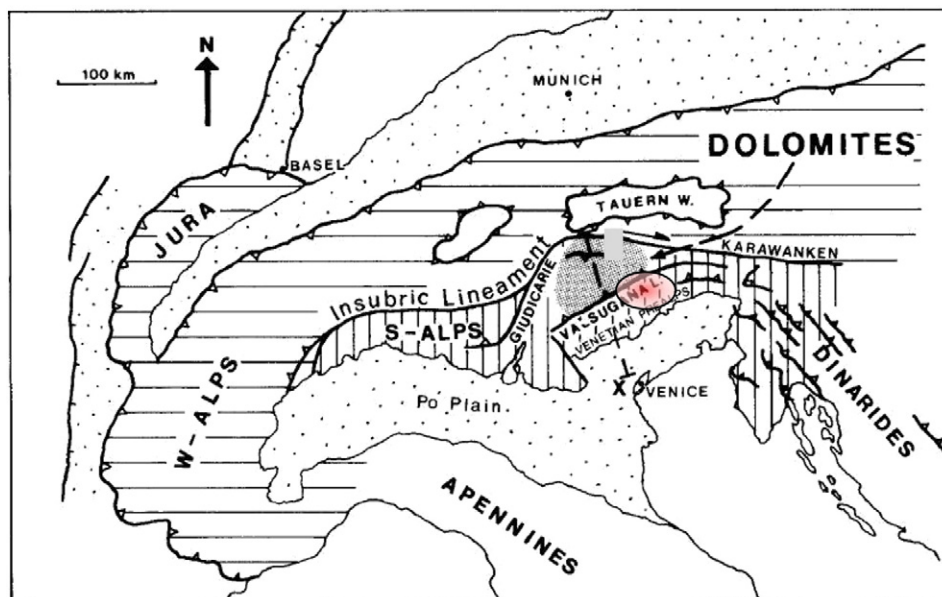

Fig. 2. Tectonic map of the Alps. The red area marks the zone of interest, in the Southern Alps domain (from Doglioni and Bosellini, 1987, modified).

may mean that geoelectric can give a fundamental contribution particularly in understanding the hillslope hydrological dynamics and the relevant impact on landslide triggering. However the two aspects of structural and hydrological characterization shall not be confused.

In the case of the Vajont landslide, a major role was played by water. Currently, though, the elevation of the water table in the landslide mass is very deep (about 200 m) and is controlled essentially by the water level in the remnant reservoir. Thus water does not play a key role in this study, and we elected to concentrate essentially on the use of seismic techniques. As we are interested in both the structure and the rock mechanical properties, we made also use of S-wave related techniques. In particular, the use of surface wave methods has been increasingly reported in the recent literature (e.g. Coccia et al., 2010; Socco et al., 2010; Renalier et al., 2010; Vignoli et al., 2012) with some particularly enlightening results, particularly for situations similar to the Vajont case (Mainsant et al., 2012). The main advantage of surface wave methods lies in their capability of identifying shear moduli that are of more direct interest in slope stability issues.

The Vajont case represents a particularly chaotic, large size landslide body that for the most part has been displaced substantially from its pre-collapse position. As a consequence, no deep geophysical seismic studies of the entire landslide body have been performed so far, also because of the difficult logistics of operating on this large landslide.

The main goal of this work is to investigate the feasibility of conducting a seismic survey under these conditions, using a variety of techniques and aiming at integrating the results into a comprehensive view of the landslide body geometry and its (current) mechanical properties. P-wave and SH-wave reflection/refraction surveys have been combined with the results of a controlled source surface wave analysis. As a result of the investigation we wish to achieve also the following practical goals:

(a) reconstruct the buried geometry of the landslide failure surface, described until now only by few data from old boreholes, and
(b) estimate the mechanical properties of the upper part of the landslide body, to be used for future geo-mechanical simulations of the event dynamics.

2. The geological setting

The study area is located in the Southeastern Alps that, including the Dolomite region, are separated from the Orogenic wedge of the Alps (s.s.) by an important fault system known as the Insubric (or Periadriatic) lineament (Fig. 2). In the Vajont valley the outcropping stratigraphic sequence goes chronologically from the Trias formation ('Dolomia Principale') to the Eocene formations (flysch). The sequence is made of the following units: 'Dolomia Principale' formation, 'Soverzene' formation, 'Igne' formation, 'Vajont' limestone, 'Fonzaso'formation, 'Soccher' formation, 'Scaglia Rossa' formation, 'Erto' marls and the Eocenic flysch. The Jurassic and Cretaceous rocks that were involved in the landslide movement (limestones and marls mainly of the Soccher and Fonzaso formations) present various degrees of fracturing. These formations slid down along the "chair-like" bedding planes, causing the outcropping of the Fonzaso formation on the Mount Toc slope (Genevois and Ghirotti, 2005). The upper part of the Fonzaso formation is characterized by a series of interbedded clay layers with variable thickness from few cm to about 3 m. The above-mentioned clay layers in the Fonzaso formation are considered one of the causes for the failure of the Vajont landslide (Hendron and Patton, 1985). This is confirmed by evidence from the existing boreholes, which show how the rock sliding surface is located precisely in the Fonzaso formation. In fact, these clayey layers seem to be continuous over a large area of the failure surface (Hendron and Patton, 1985), as shown in Fig. 3.
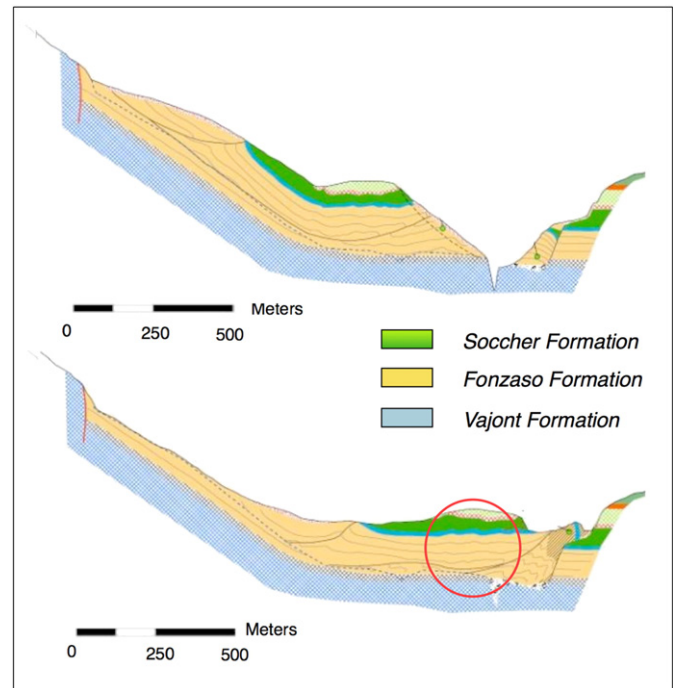

Fig. 3. Schematic section of the Mount Toc slope before and after the 1963 landslide, as reported by Rossi and Semenza (1965), modified. The red circle indicates the area investigated in this study. Note that the landslide failure surface is confined in the Fonzaso formation.

3. The geophysical surveys

We performed an intense geophysical survey program on the Vajont landslide body in the Spring of 2011. The aim of the investigation was primarily to test the feasibility and effectiveness of a number of seismic methods to study such a large and complex landslide environment. Two reflection seismic lines with a vibrator source, both for P waves and SH waves' orientations, were collected on the top of the landslide body (L1 and L2 in Fig. 4). One surface wave seismic survey with a heavy drop-weight source and low frequency receivers was collected along part of line L1.

In the 1960s, shortly after the slide event, several boreholes were drilled in the landslide body but unfortunately most of the data appear
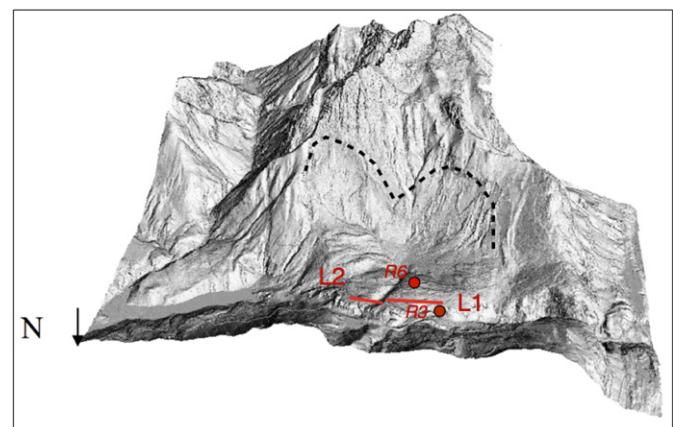

Fig. 4. Geophysical surveys localized onto a Lidar image of the Mount Toc. Note on the map the large scar left by the landslide (marked by the dotted black line). The seismic lines L1 and L2 are shown in red. R3 and R6 are existing post-event boreholes used for correlation with the seismic data.

Table 1
Acquisition parameters of the reflection seismic lines on the Vajont landslide body.

P-wave reflection survey	
Line L1	
Seismic source	MiniVib P-wave mode
Channel number (fixed spread)	256
Receiver	Single 10 Hz vertical geophone
Channel interval	2 m
Total length	510 m
Sampling rate	1 ms
Shot interval	4 m
Shot points	125
Line L2	
Seismic source	MiniVib P-wave mode
Channel number (fixed spread)	162
Receiver	Single 10 Hz vertical geophone
Channel interval	2 m
Total length	322 m
Sampling rate	1 ms
Shot interval	4 m
Shot points	81
SH-wave reflection survey	
Line L1	
Seismic source	MiniVib SH-wave mode
Channel number (fixed spread)	113
Receiver	Single 10 Hz horizontal geophone
Channel interval	4 m
Total length	448 m
Sampling rate	1 ms
Shot interval	8 m
Shot points	50

Table 2
Seismic reflection processing flow for the reflection seismic data.

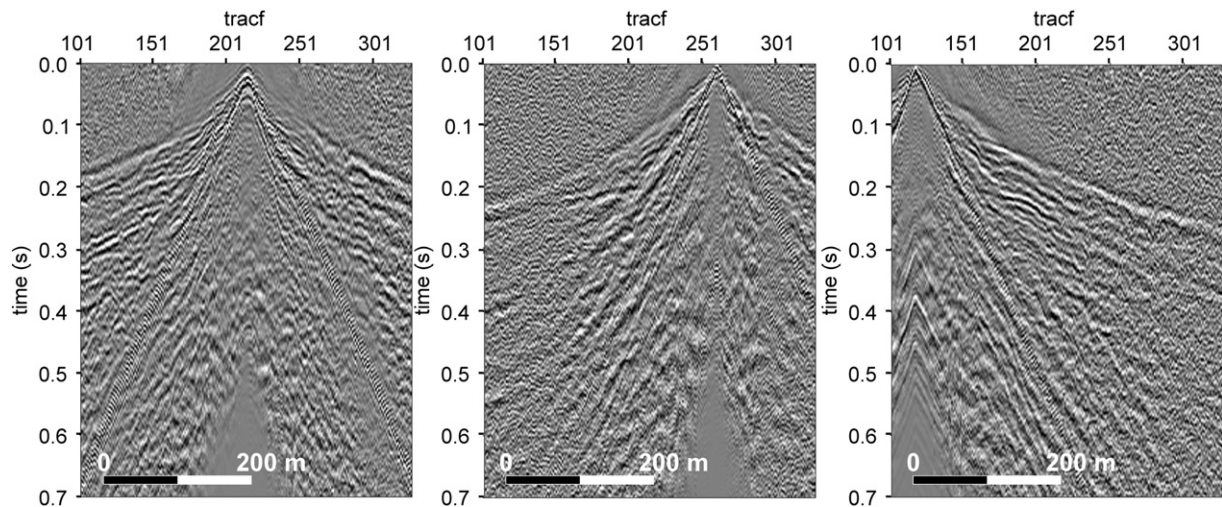|	
1	Format from SEG2 to SU
2	Cross-correlation with ground force signal
3	Preliminary editing
4	Vertical stacking
5	Assign geometries (input source and receiver locations)
6	First arrival picking
7	Spherical divergence recovery
8	Predictive deconvolution
9	First arrivals muting
10	Frequency filtering
11	Surgical muting (removal of ground-roll)
12	Static correction
13	Notch filter (50 Hz only for bad trace)
14	Sort into CDPs (re-order traces in common midpoints) and binning
15	Velocity analysis
16	NMO correction (semblance)
17	CDP stack

introducing a redundant information content, mandatory for applications on such highly heterogeneous and noisy fields. The seismic line acquisition parameters for P- and SH-wave surveys are reported in Table 1,

The reflection analysis on single common P wave shot gather highlighted complex wavefields. Beyond first arrivals, clearly observable even at large offsets (400 to 500 m), a significant ground roll is present (see e.g. Fig. 5). Outside the ground roll cone reflected events are detectable in many P-wave common-shot gathers, even if they present complex patterns and limited lateral continuity. SH-wave data are contaminated by strong ground roll and they are not processed for reflections.

In the first step, P wave data were processed by a conventional processing sequence (Table 2) with a pre-stack signal enhancement and a subsequent cdp stacking. Subsequently a prestack Kirchhoff time migration was applied to improve the continuity of the horizons and to obtain a better seismic imaging (Fig. 6). The velocity model was derived by a lateral interpolation of the vertical velocity functions picked in the semblance spectra during the velocity analysis for the NMO correction. The same model was also used to perform the depth conversion of the P-wave L1 line.

Clear first arrivals were detected both in P- and SH-waves' dataset so a preliminary P wave and SH wave velocities were computed from the first arrivals of the L1 recordings. Fig. 7 shows the first arrival pickings performed on P- and SH-wave respectively. Direct modeling was adopted to obtain simplified 1D velocity models for depth conversion of the refraction data (Fig. 7).

to be lost (Superchi et al., 2010). In the studied area only 2 boreholes drilled in 1964 have been identified with reliable stratigraphic descriptions (R3 and R6 in Fig. 4). These data were then considered for comparison with the seismic results.

3.1. Seismic reflection acquisition

The very limited access conditions to the landslide body, especially in terms of seismic source vehicle movement, drove the choice for the locations of the acquisition lines. The landslide body surface has a very irregular topography and is very heterogeneous in terms of outcropping materials. To overcome the logistic problems we adopted a large number of recording channels with short trace interval in a fixed spread configuration. This approach allowed us to obtain an investigation with a very high spatial density, thus

Fig. 5. Seismic line L1: examples of common shot-gathers (P-wave source and vertical geophones).
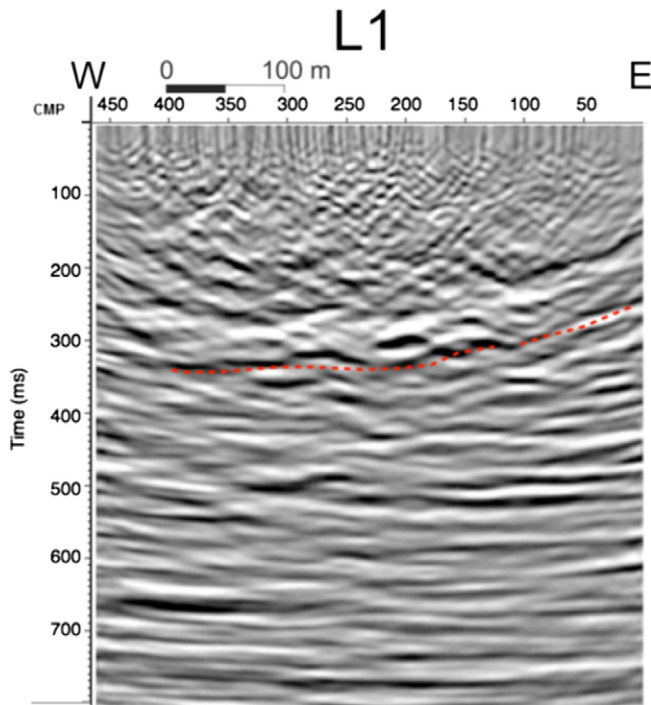
Fig. 6. Seismic line L1: example of Kirchhoff pre-stack time migration. The red dashed lines mark the main visible reflection (see Section 5 for discussion).

3.2. Surface wave acquisition

One of the aim of this study was to obtain a shear wave velocity (V_S) profile of the Vajont landslide body. This, together with estimates of P-wave velocity (V_P) from first arrival refractions, allows the estimation of in-situ Poisson's ratio, that in turn can be compared against laboratory measurements on rock samples.

In order to overcome the limitations in detecting velocity coming from usual SH prospecting, we also adopted surface wave analyses. In particular the method was applied to enhance the inversion of S-wave velocity in the upper Soccher formation.

The surface wave survey was performed by the use of a weight-drop controlled source, using a 250 kg weight released by the arm of a crane at 6, 10 and 14 m above ground at 9 different locations along line L1 (Fig. 8). We performed both MASW analysis (Multi-channels Analysis of Surface Waves, Park et al., 1999; Foti et al., 2014) and FTAN analysis (Frequency–Time Analysis, Dziewonski et al., 1969; Levshin et al., 1972; Knopoff and Panza, 1977; Nunziata et al., 1999; Boaga, 2013).

For the MASW approach the seismic signals were recorded by 48 vertical geophones with a natural frequency of 4.5 Hz with 4 m trace intervals, along the first portion of line L1. For the FTAN methods the weight drop signals were recorded by 3 low-frequency vertical receivers with natural period of 1 s, located at fixed positions from the source (100 m, 200 m and 510 m). MASW data were inverted using the SWAMI code (Lai and Rix, 1998), while for FTAN data the Hedgehog non-linear inversion was adopted (Valyus et al., 1968; Panza, 1981). Given the current field conditions and source frequency range, MASW data are estimated to reach an exploration depth of 60 m ($\lambda \approx 120$ m) while the FTAN method, based on few lower frequency receivers, likely reached 130 m ($\lambda \approx 260$ m) in depth (Fig. 9).

Given the different penetration depths of the two surface-wave methods, we assumed as a representative 1D vertical VS profile the one obtained by combining MASW results in shallower layers and FTAN results for the deeper structure (see Section 4 for details).

4. Results

Fig. 10 shows the P-wave and S-wave velocity profiles, as derived from the seismic refraction analysis (using P waves and SH waves) and from the surface wave analysis. The figure shows also the Poisson's ratio as estimated on site from the seismic measurements and the Poisson's ratio as derived from laboratory measurements on a number of Vajont rocks specimens (Ferri et al., 2010). Fig. 10 shows that the V_S estimated from surface waves and the V_S from SH profiling along the same portion of line L1 are in good agreement. Both profiles show a low velocity upper part (referred to the deep fractured Soccher formation) followed by a sharp velocity increase at around 80 m depth.
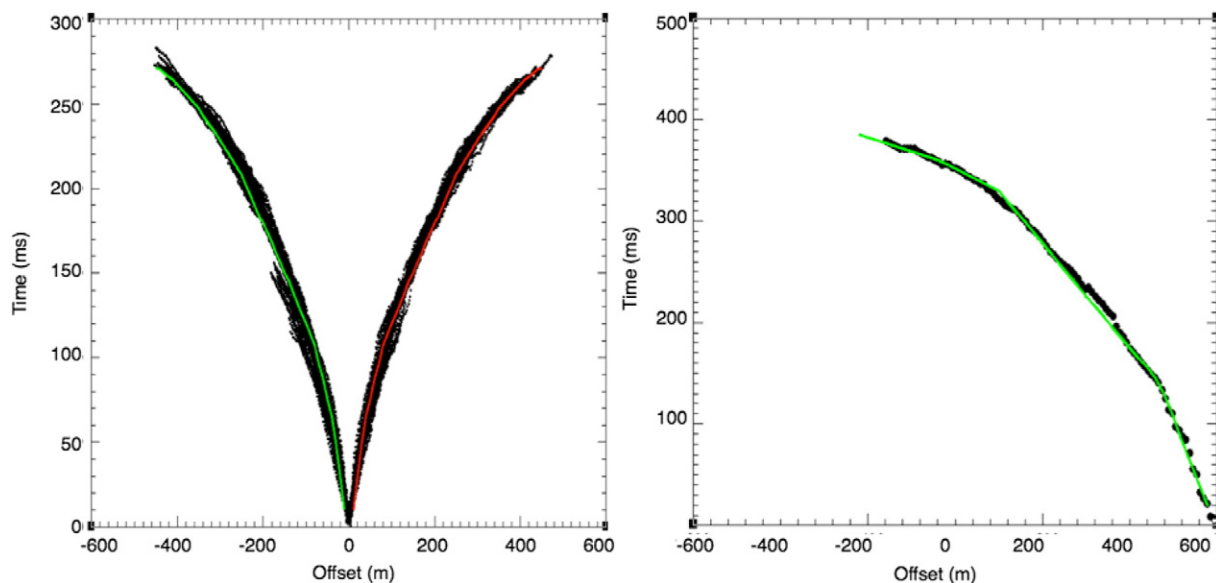

Fig. 7. L1 first break picking for P-waves (on the left side) and SH waves (on the right side). Black points corresponds to the measured data while red and green lines represent the computed first arrivals obtained by a simplified 1 D models for P- and SH-wave velocities.

Fig. 8. The weight-drop apparatus used for surface wave surveys.

Surface wave V_S results also show an interesting velocity inversion between 40 and 60 m in depth. This layer is not visible from SH refraction, since velocities inversion cannot be seen by layer-based refraction methods for intrinsic limitations. This inversion can play a relevant role in mechanical interpretation of the landslide event.

The in-situ estimated Poisson's ratios are in general agreement with laboratory measurements, showing a low value corresponding to the lower Fonzaso formation at 160 m depth.

Fig. 11 shows the depth converted L1 seismic line with a line drawing of the main visible reflections. Here we considered the L1 seismic line results for the presence of the R3 borehole data for comparison. There are several minor reflections and intense scattering, as expected in such a chaotic landslide environment, and one main, although fairly discontinuous, reflector located between 160 m and 110 m in depth from the western part to the eastern part respectively.

Fig. 12 shows a summary of the results along section L1 with the line drawing of main P reflections together with the obtained velocity profiles and the R3 borehole simplified stratigraphy. We show only R3 borehole data because it is closer to the seismic line than R6 (Fig. 2) and because the two boreholes present very similar stratigraphy.

The shallower low velocities zone, including the V_S inversion layer, is likely to be related to the partially fractured Soccher formation, while the sharp increase in velocity at 80 m depth can be related to the transition between the Soccher formation and the less fractured Fonzaso upper formation (Superchi, 2010).

The main identified reflection surface is located, sloping from East to West, between 110 and 160 m depth, seems to be related to the upper and lower Fonzaso formation limit, where there is an increment also in V_P velocity values. This zone was reported in the borehole description as the recognized landslide failure surface.
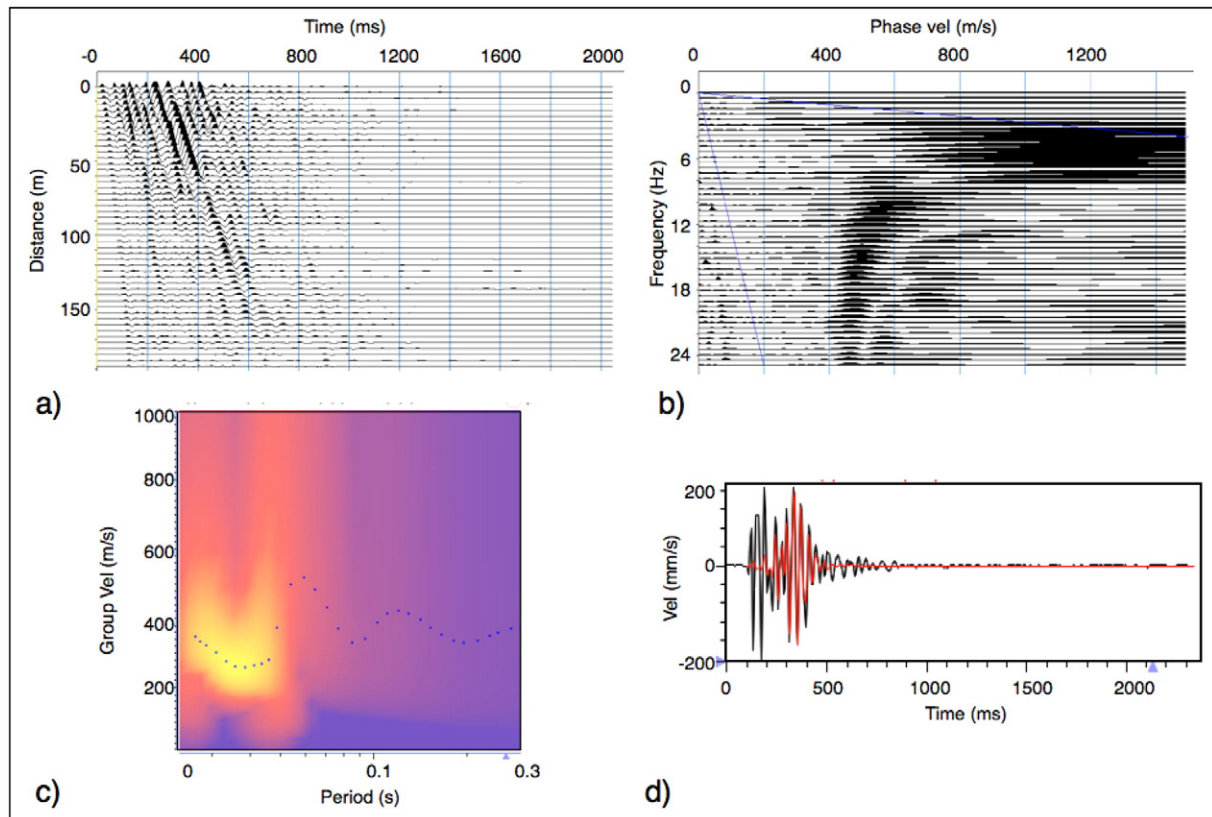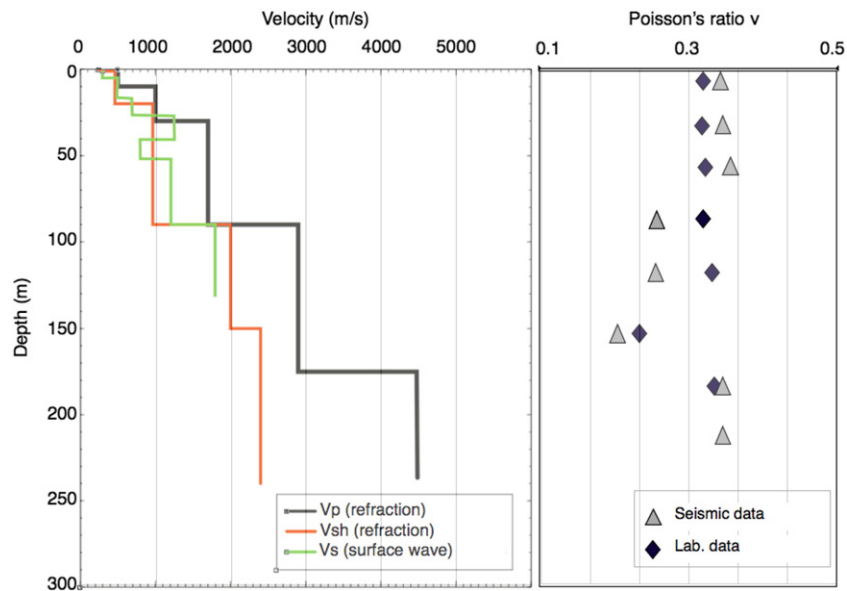

Fig. 9. Examples of surface wave analysis on the Vajont landslide body: a) a MASW record and b) the corresponding P–F spectrum; c) example of FTAN map and d) the corresponding vertical low frequency receiver recorded signal (black) and the extracted signal selected from the FTAN map as the fundamental mode (red).

Fig. 10. a) 1D velocities profiles as derived from seismic (P and SH) refraction surveys and surface wave analysis. Note that the surface wave method produces an inversion of V_S velocities between 40 and 60 m in depth that cannot be detected by the refraction methods. Two sharp velocity increases are visible at 80 m and at 170 m depth. b) Poisson's ratio as derived from the seismic surveys and from laboratory measurements on Vajont rock specimens (Ferri et al., 2010). Note the low Poisson's ratio in the Fonzaso formation at 160 m depth, and confirmed by both in situ and laboratory estimates.

5. Discussion, interpretation and conclusions

The combined seismic surveys conducted on the Vajont landslide body allowed us to reconstruct the subsoil main geometries and to characterize the mechanical properties of the rockmass. Fig. 13 summarizes the reconstruction of the landslide body compared against borehole data, the obtained velocity profiles and the geological interpretation. The first sharp increase of the seismic velocities at depth is interpreted as the contact between the Soccher and the upper Fonzaso formations, which the B3 borehole stratigraphy identifies at 70 m depth. The low velocities found in the shallower layers can be associated to the deeply fractured Soccher formation, which is characterized by a sequence of fractured limestone and marls. The low V_S velocity layer detected by the surface wave analysis can be related to the presence of a thick marls level within the Soccher formation (Superchi, 2010). The retrieved velocities are consistent with the expected properties of these fractured rocks (Ferri et al., 2010). For this upper part of the landslide, the comparison between the Poisson's ratio estimated on site by the shear and compressional wave velocities and the one obtained with laboratory tests on specimens, can play a relevant role in future mechanical interpretation (compare e.g. with Palchik, 2011). In particular our results, in terms of landslide seismic characterization, support the most recent reconstruction of the landslide dynamic (see Wolter et al., 2013; Stead and Eberhardt, 2013), addressing a failure surface at ca. 150 m depth from the actual topographic surface. On the contrary our study highlights the unlikely reconstruction of some authors
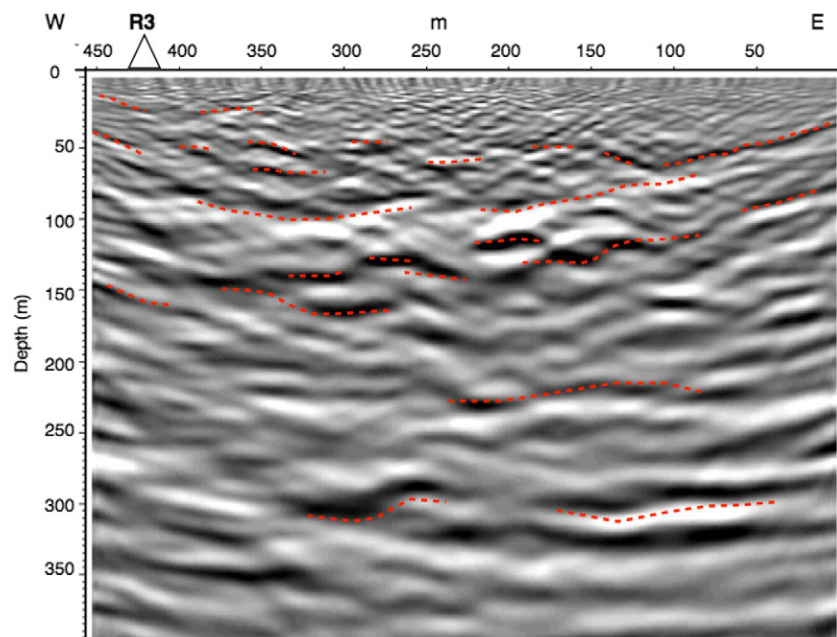
Fig. 11. L1 depth section with the line drawing of the main visible reflections. The R3 borehole that can be used for comparison is located in the western part of the section.
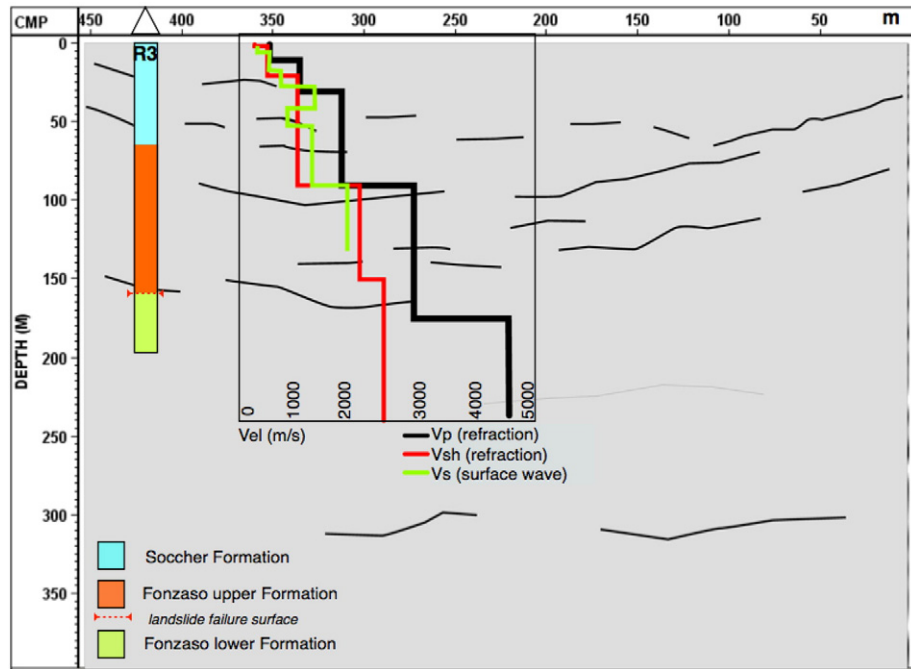
Fig. 12. Line drawing of the main reflections in line L1, compared against the V_P and V_S velocity profiles and the schematic stratigraphy from the 1964 R3 borehole. The dotted red line in the R3 borehole is the recognized failure surface from borehole information.

(Hendron and Patton, 1985; Trollope, 1980; Alonso, 2010), which consider deeper failure surface and consequently different mass involved in the failure process. For these reasons the conducted seismic characterization will play a relevant role in the future geo-mechanical reconstruction of the Vajont landslide.

The main visible reflector in the reflection sections can be in fact interpreted as the landslide failure surface. As described by the borehole data it is in fact located at a maximal depth of about 160 m in this area.

The hypothesis that the sliding surface corresponds to the limit between upper and lower Fonzaso formation seems to be verified by the presence of the main reflector smoothly increasing in depth from West to East, from 160 to 110 m below the ground surface.

The very detailed seismic surveys were conducted in very difficult subsurface conditions, with chaotic buried structures and surface scattering, posing challenging issues about quality of the data. Nevertheless the huge amount of reflection/refraction data, together with surface
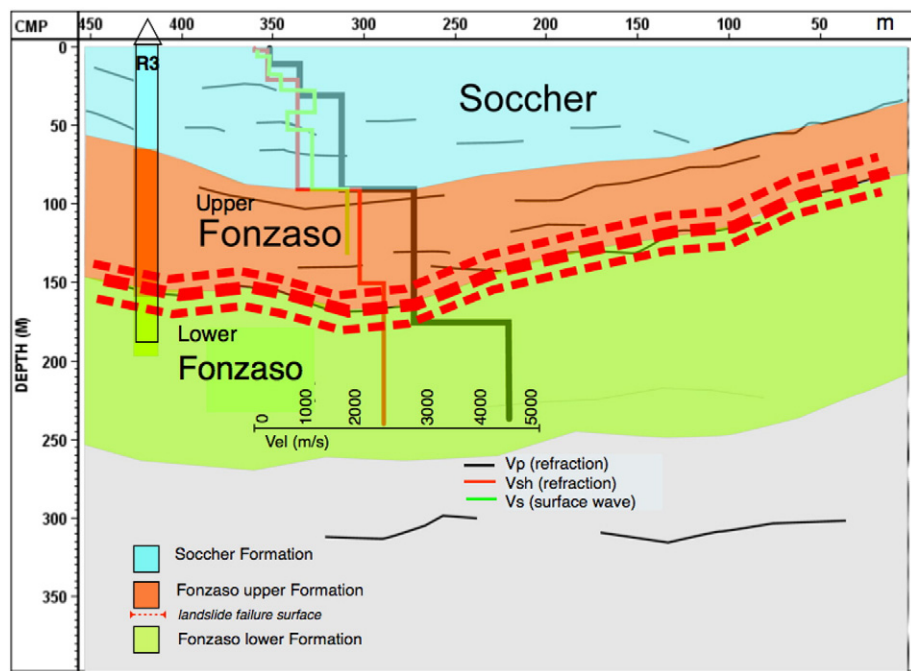
Fig. 13. Interpretation of seismic line L1. R3 is the 1964 borehole used for correlation. In blue the Soccher formation; in orange the upper Fonzaso formation, in green the lower Fonzaso formation. Velocities profiles (are as above) V_P in black line, V_S in red line, both from first arrival refractions. The green line shows the V_S profile derived from surface waves. The dashed thick red line marks the interpreted main sliding surface.

wave analyses, allowed us to characterize the seismic properties of the Vajont landslide mass.

These results are particularly good, considering also the logistical challenges of this large landslide. In fact, even though the site only allows sub-optimal geophones ground coupling and limited sources deployment, the geophysical surveys show good agreement with borehole data and allow a 2D imaging of the landslide shear zone. These good quality results could be achieved by using a large number of active channels, together with short receiver intervals and adequate seismic sources. In addition, the joint use of refraction seismic and surface wave methods considerably improve the estimation of subsoil mechanical properties, and are for these reasons promising tools to be used in similar situations.

Acknowledgments

References

Alonso, A., 2010. Geomechanics of failures. Advanced Topics. © Springer http://dx.doi.org/10.1007/978-90-481-3538-7_2.

Bievre, G., Jongmans, D., Winiarski, T., Zumbo, V., 2012. Application of geophysical measurements for assessing the role of fissures in water infiltration within a clay landslide (Trieves area, French Alps). Hydrol. Process. 26 (14), 2128–2142 (Special Issue: SI).

Boaga, J., 2013. An efficient tool for cultural heritage seismic soil classification: frequency time analysis method in Venice historical center and its lagoon (Italy). Geosci. J. 17 (3), 301–311.

Boyer, R.A., 1913. Etude géologique des environs de Longarone (Alpes Vénitiennes). Bull. Soc. Geol. Fr. 13, 451–485 (A027).

Carloni, G.C., Mazzanti, R., 1964a. Rilevamento geologico della frana del Vaiont. Giorn. Geol. XXXII (I), 105–138.

Carloni, G.C., Mazzanti, R., 1964b. Aspetti geomorfologici della frana del Vaiont. Riv. Geogr. Ital. 71 (3), 201–231.

Carpentier, S., Konz, M., Fischer, R., Anagnostopoulos, G., Meusburger, K., Schoeck, K., 2012. Geophysical imaging of shallow subsurface topography and its implication for shallow landslide susceptibility in the Urseren Valley, Switzerland. J. Appl. Geophys. 83 (2012), 46–56. http://dx.doi.org/10.1016/j.jappgeo.2012.05.001.

Coccia, S., Del Gaudio, V., Venisti, N., Wasowski, J., 2010. Application of refraction Microtremor (ReMi) technique for determination of 1-D shear wave velocity in a landslide area. J. Appl. Geophys. 71 (2010), 71–89. http://dx.doi.org/10.1016/j.jappgeo.2010.05.001.

Dal Piaz, G. (1928). Relazione di massima su due sezioni del Vajont prese in considerazione per progetti di sbarramento idraulico. Unpublished technical report for S.A.D.E., Venezia, Italy.

De Vita, P., Agrello, D., Ambrosino, F., 2006. Landslide susceptibility assessment in ash-fall pyroclastic deposits surrounding Mount Somma-Vesuvius: application of geophysical surveys for soil thickness mapping. J. Appl. Geophys. 59 (2006), 126–139. http://dx.doi.org/10.1016/j.jappgeo.2005.09.001.

Doglioni, C., Bosellini, A., 1987. Eoalpine and mesoalpine tectonics in the Southern Alps. Geol. Rundsch. 76 (3), 735–754.

Dziewonski, A., Bloch, S., Landisman, M., 1969. A technique for the analysis of transient seismic signals. Bull. Seismol. Soc. Am. 59, 427–444.

Ferri, F., Di Toro, G., Hirose, T., Shimamoto, T., 2010. Evidence of thermal pressurization in high-velocity friction experiments on smectite-rich gouges. Terra Nova 22, 347–353.

Foti, S., Lai, C.G., Rix, G.J., Strobbia, C., 2014. Surface Wave Methods for Near-surface Site Characterization. CRC Press 9780415678766 (487 pp.).

Frattini, M., Arredi, F., Boni, A., Fasso, C., Scarsella, F., 1964. Relazione sulle cause che hanno determinato la frana nel serbatoio del Vajont (9 Ottobre 1963). Frattini Commission Report Prepared for ENEL. Roma (92 pp.).

Gance, J., Grandjean, G., Samyn, K., Malet, J.-P., 2012. Quasi-Newton inversion of seismic first arrivals using source finite bandwidth assumption: application to subsurface characterization of landslides. J. Appl. Geophys. 87 (2012), 94–106. http://dx.doi.org/10.1016/j.jappgeo.2012.09.008.

Genevois, R., Ghirotti, M., 2005. The 1963 Vaiont landslide. G. Geol. Appl. 1, 41–52.

Godio, A., Bottino, G., 2001. Electrical and electromagnetic investigation for landslide characterization. Phys. Chem. Earth 26, 705–710.

Godio, A., Strobbia, C., De Bacco, G., 2006. Geophysical characterisation of a rockslide in an alpine region. Eng. Geol. 83, 273–286.

Göktürkler, G., Balkaya, C., Erhan, Z., 2008. Geophysical investigation of a landslide: the Altındağ landslide site, İzmir (western Turkey). J. Appl. Geophys. 65 (2008), 84–96. http://dx.doi.org/10.1016/j.jappgeo.2008.05.008.

Grandjean, G., Gourry, J.C., Sanchez, O., Bitri, A., Garambois, S., 2011. Structural study of the Ballandaz landslide (French Alps) using geophysical imagery. J. Appl. Geophys. 75 (2011), 531–542. http://dx.doi.org/10.1016/j.jappgeo.2011.07.008.

Heincke, B., Maurer, H., Green, A.G., Willenberg, H., Spillmann, T., Burlini, L., 2006. Characterizing an unstable mountain slope using shallow 2D and 3D seismic tomography. Geophysics 71 (6), B241–B256. http://dx.doi.org/10.1190/1.2338823 (NOVEMBER–DECEMBER 2006).

Heincke, B., Günther, T., Dalsegg, E., Rønning, J.S., Ganerød, G.V., Elvebakk, H., 2010. Combined three-dimensional electric and seismic tomography study on the Åknes rockslide in western Norway. J. Appl. Geophys. 70 (2010), 292–306. http://dx.doi.org/10.1016/j.jappgeo.2009.12.004.

Hendron, A.J., Patton, F.D., 1985. The Vaiont slide, a geotechnical analysis based on new geologic observations of the failure surface. Technical Report GL-85-5. U.S. Army Engineer Waterways Experiment Station, Vicksburg, MS. I, II.

Jongmans, D., Garambois, S., 2007. Geophysical investigation of landslide: a review. Bull. Fr. Geol. Soc. 178 (2), 101–112.

Jongmans, D., Hembrouille, P., Demanet, D., Renardy, F., Vanbrabant, Y., 2000. Application of 2D electrical and seismic tomography techniques for investigating landslides. Eur. J. Environ. Eng. Geophys. 5, 75–89.

Kiersch, G.A., 1964. Vaiont reservoir disaster. Civ. Eng. 34 (3), 32–39.

Knopoff, L., Panza, G.F., 1977. Resolution of upper mantle structure using higher modes of Rayleigh waves. Ann. Geophys. 30, 491–505.

Lai, C.G., Rix, G.J., 1998. Simultaneous inversion of Rayleigh phase velocity and attenuation for near-surface site characterization. Report No. Git-Cee/Geo-98-2. School of Civil and Environmental Engineering, Georgia Institute of Technology (258 pp.).

Lapenna, V., Lorenz, P., Perrone, A., Piscitelli, S., Rizzo, E., Sdao, F., 2005. 2D electrical resistivity imaging of some complex landslides in the Lucanian Apennine chain, southern Italy. Geophysics 70 (3), B11–B18. http://dx.doi.org/10.1190/1.1926571 (MAY–JUNE).

Levshin, A., Pisarenko, V.F., Pogrebinsky, G.A., 1972. On a frequency–time analysis of oscillations. Ann. Geophys. t.28 (fasc.2), 211–218.

Mainsant, G., Larose, E., Broennimann, C., Jongmans, D., Michoud, C., Jaboyedoff, M., 2012. Ambient seismic noise monitoring of a clay landslide: toward failure prediction. J. Geophys. Res. Earth Surf. 117, F01030 (Published: MAR 22, 2012).

Malehmir, A., Saleem, M.U., Bastani, M., 2013. High-resolution reflection seismic investigations of quick-clay and associated formations at a landslide scar in southwest Sweden. J. Appl. Geophys. 92 (2013), 84–102. http://dx.doi.org/10.1016/j.jappgeo.2013.02.013.

Mantovani, F., Vita-Finzi, C., 2003. Neotectonics of the Vajont dam site. engineering. Geomorphology 54 (1–2), 33–37.

Müller, L., 1964. The rock slide in the Vaiont valley. Rock Mech. Eng. Geol. 2, 148–212.

Müller, L., 1968. New considerations on the Vaiont slide. Rock Mech. Eng. Geol. 6, 1–91 (Contains experimental data, A044).

Müller, L., 1987. The Vaiont slide. Eng. Geol. 24, 513–523. http://dx.doi.org/10.1016/0013-7952(87)90082-2 (In: Leonards G.A. (ed) — Dam failures, http://www.sciencedirect.com/science/journal/00137952, A050).

Nguyen, F., Garambois, S., Chardon, D., Hermitte, D., Bellier, O., Jongmans, D., 2007. Subsurface electrical imaging of anisotropic formations affected by a slow active reverse fault, Provence, France. J. Appl. Geophys. 62 (4), 338–353 (Published: AUG 2007).

Nunziata, C., Costa, G., Natale, M., Panza, G.F., 1999. FTAN and SASW methods to evaluate Vs of neapolitan pyroclastic soils. Earthquake Geotechnical Engineering, 1. Balkema, P.

Palchik, V., 2011. On the ratios between elastic modulus and uniaxial compressive strength of heterogeneous carbonate rocks. Rock Mech. Rock. Eng. 44, 121–128.

Panza, G.F., 1981. The resolving power of seismic surface waves with respect to the crust and upper mantle structural models. In: Cassinis, R. (Ed.), The Solution of the Inverse Problem in Geophysical Interpretation. Plenum Publishing Corporation, pp. 39–77 (p. 15–19).

Park, C.B., Miller, R.D., Xia, J., 1999. Multi-channel analysis of surface waves. Geophysics 64 (3), 800–808.

Piegari, E., Cataudella, V., Di Maio, R., Milano, L., Nicodemi, M., Soldovieri, M.G., 2009. Electrical resistivity tomography and statistical analysis in landslide modelling: a conceptual approach. J. Appl. Geophys. 68 (2009), 151–158. http://dx.doi.org/10.1016/j.jappgeo.2008.10.014.

Renalier, F., Jongmans, D., Campillo, M., Bard, P.-Y., 2010. Shear wave velocity imaging of the Avignonet landslide (France) using ambient noise cross correlation. J. Geophys. Res. Earth Surf. 115, F03032 (Published: SEP 11, 2010).

Romdhane, A., Grandjean, G., Brossier, R., al Rejiba, F., Operto, S., Virieux, J., 2011. Shallow-structure characterization by 2D elastic full-waveform inversion. Geophysics 76 (3), R81–R93. http://dx.doi.org/10.1190/1.3569798 (MAY–JUNE 2011).

Rossi D, Semenza E (1965). Carte geologiche del versante settentrionale del M. Toc e zone limitrofe, prima e dopo il fenomeno di scivolamento del 9 Ottobre 1963, Scala 1: 5000. Istituto Geologia, University of Ferrara.

Samyn, K., Travelletti, J., Bitri, A., Grandjean, G., Malet, J.-P., 2012. Characterization of a landslide geometry using 3D seismic refraction traveltime tomography: the La Valette landslide case history. J. Appl. Geophys. 86 (2012), 120–132. http://dx.doi.org/10.1016/j.jappgeo.2012.07.014.

Schmutz, M., Guérin, R., Andrieux, P., Maquaire, O., 2009. Determination of the 3D structure of an earth flow by geophysical methods. the case of Super Sauze, in the French Southern Alps. J. Appl. Geophys. 68 (2009), 500–507. http://dx.doi.org/10.1016/j.jappgeo.2008.12.004.

Semenza, E., 1986. New geological studies on the Vaiont area. In: Semenza, E., Melidoro, G. (Eds.), Proceedings of the Meeting on the 1966 Vaiont Landslide, Convegno Sulla Frana del Vaiont, 199–213, Università di Ferrara, Italy, 17–19 September 1986, p. C024.

Semenza, E., 2010. The Story of Vaiont Told by the Geologist Who Discovered the Landslide, K-Flash Ed. p. 205.

Semenza, E., Ghirotti, M., 1998. Vaiont–Longarone 34 anni dopo la catastrofe. Annali dell'Università di Ferrara (Nuova Serie). Sezione Sci. Terra 7 (4), 63–94.

Socco, L.V., Jongmans, D., Boiero, D., Stocco, S., Maraschini, M., Tokeshi, K., Hantz, D., 2010. Geophysical investigation of the Sandalp rock avalanche deposits. J. Appl. Geophys. 70 (2010), 277–291. http://dx.doi.org/10.1016/j.jappgeo.2009.12.005.

Stead, D., Eberhardt, Erik E., 2013. Understanding the mechanics of large landslides. Proc. International Conference on Vajont—1963–2013, Padova, Italy.

Stucchi, E., Mazzotti, A., 2009. 2D seismic exploration of the Ancona landslide (Adriatic Coast, Italy). Geophysics 74 (5), B139–B151. http://dx.doi.org/10.1190/1.3157461 (SEPTEMBER–OCTOBER).

Superchi, L.V., 2010. The Vajont landslide rockslide: new techniques and traditional methods to re-evaluate the catastrophic event PhD Thesis Università di Padova, Italy.

Superchi, L., Floris, M., Ghirotti, M., Genevois, R., Jaboyedoff, M., Stead, D., 2010. Implementation of a geodatabase of published and unpublished data on the catastrophic Vaiont landslide. Nat. Hazards Earth Syst. Sci. 10, 865–873.

Suzuki, K., Higashi, S., 2001. Groundwater flow after heavy rain in landslide-slope area from 2-D inversion of resistivity monitoring data. Geophysics 66 (3), 733–743 (MAY–JUNE 2001).

Tric, E., Lebourg, T., Jomard, H., Le Cossec, J., 2010. Study of large-scale deformation induced by gravity on the La Clapière landslide (Saint-Etienne de Tinée, France) using numerical and geophysical approaches. J. Appl. Geophys. 70 (2010), 206–215. http://dx.doi.org/10.1016/j.jappgeo.2009.12.008.

Trollope, D.H., 1980. The Vajont slope failure. Rock Mechanics Vol. 13. Springer, pp. 71–88.

Valyus, V.P., Keylis-Borok, V.I., Levshin, A.L., 1968. Determination of the velocity profile of the upper mantle. Eur. Nauk SSSR 185 (8), 564–567.

Vignoli, G., Cassiani, G., Rossi, M., Deiana, R., Boaga, J., Fabbri, P., 2012. Geophysical characterization of a small pre-alpine catchment. J. Appl. Geophys. 80, 32–42. http://dx.doi.org/10.1016/j.jappgeo.2012.01.007.

Wolter, A., Havaej, M., Zorzi, L., Stead, D., Clague, J.J., et al., 2013. Exploration of the kinematics of the 1963 Vajont slide, Italy, using a numerical modelling toolbox. Ital. J. Eng. Geol. Environ. (TOPIC 6).